Published online 29 November 2007

Nucleic Acids Research, 2008, Vol. 36, No. 2 ***511–519***
doi:10.1093/nar/gkm1052

ATR-dependent pathways control hEXO1 stability in response to stalled forks

Mahmoud El-Shemerly[1], Daniel Hess[2], Aswin K. Pyakurel[1], Said Moselhy[1] and Stefano Ferrari[1,*]

[1]Institute of Molecular Cancer Research, University of Zurich, Winterthurerstrasse 190, CH-8057 Zurich and [2]Friedrich Miescher Institute for Biomedical Research, Maulbeerstrasse 66, CH-4058 Basel, Switzerland

Received October 18, 2007; Accepted November 5, 2007

ABSTRACT

Nucleases play important roles in DNA synthesis, recombination and repair. We have previously shown that human exonuclease 1 (hEXO1) is phosphorylated in response to agents stalling DNA replication and that hEXO1 consequently undergoes ubiquitination and degradation in a proteasome-dependent manner. In the present study, we have addressed the identity of the pathway transducing stalled-replication signals to hEXO1. Using chemical inhibitors, RNA interference, ATM- and ATR-deficient cell lines we have concluded that hEXO1 phosphorylation is ATR-dependent. By means of mass spectrometry, we have identified the sites of phosphorylation in hEXO1 in undamaged cells and in cells treated with hydroxyurea (HU). hEXO1 is phosphorylated at nine basal sites and three additional sites are induced by HU treatment. Analysis of single- and multiple-point mutants revealed that mutation to Ala of the three HU-induced sites of phosphorylation partially rescued HU-dependent degradation of hEXO1 and additionally stabilized the protein in non-treated cells. We have raised an antibody to pS_{714}, an HU-induced site of the S/T-Q type, and we provide evidence that S_{714} is phosphorylated upon HU but not IR treatment. The antibody may be a useful tool to monitor signal transduction events triggered by stalled DNA replication.

INTRODUCTION

Exonuclease 1 is a DNA repair nuclease of the Rad2 family originally identified in the fission yeast *Schizosaccharomyces pombe* (1). The activity of *S. pombe Exo1* gene product is induced about 5-fold just prior to meiosis, which led to the suggestion that Exo1 might be involved in meiotic homologous recombination (1). Transcriptional induction of the *Saccharomyces cerevisiae* and the *Drosophila melanogaster EXO1* gene during meiosis has also been reported (2,3). Mouse Exo1 was found predominantly expressed in testis and the spleen, consistent with roles in processes specific to germ cell maturation and hematopoiesis (4). The human homolog *EXO1* gene encodes a protein bearing only 27% identity to its yeast counterpart (5,6). Nonetheless, human exonuclease 1 (hEXO1) was shown to be functionally similar to the yeast protein by its ability to complement *S. cerevisiae* Exo1 and the mutator phenotype of the yeast *rad27* mutant (5,7). In humans, two isoforms (hEXO1a and hEXO1b) have been described to arise from alternative splicing (5,8), though no functional differences between the two isoforms have been reported. The expression of hEXO1 reflects the pattern reported for the mouse, with high levels in testis, thymus and colon and slightly lower expression in small intestine, placenta, spleen and ovary (5).

EXO1 catalyzes the removal of mononucleotides from the 5′ end of the DNA duplex, showing a strong preference for blunt-ended, 5′ recessed termini and DNA nicks. It can also degrade exonucleolytically single-stranded DNA, although less efficiently than double-stranded DNA (9,10). Moreover, hEXO1 displays a 5′ ssDNA-flap-specific endonuclease activity but does not possess endonuclease activity at bubble-like structures (10).

In *S. cerevisiae*, EXO1 was shown to participate in meiotic crossing over as well as in the processing of double-strand breaks (DSB) ends (2). An additional role in mutation avoidance and mismatch correction was described for *S. pombe* Exo1 (11). Mismatch repair (MMR) is a mechanism reducing the rate of somatic microsatellite polymorphism and it is disabled in a number of human cancers (12). The involvement of Exo1 in MMR was confirmed by studies demonstrating

*To whom correspondence should be addressed. Tel: +41 44 635 3471; Fax: +41 44 635 3484; Email: sferrari@imcr.uzh.ch
Present address:
Said Moselhy, Department of Biochemistry, Faculty of Science, Aim-Shams University, Abbassia, Cairo, Egypt.

physical and genetic interaction between yeast Exo1 and the MMR proteins Msh2 (6) and Mlh1 (13). Furthermore, an independent study confirmed the structural role of yeast Exo1 in the stabilization of the multiprotein complex containing MMR proteins (14). Studies conducted with human recombinant proteins or HeLa cells extracts confirmed the interaction between hEXO1 and the MMR proteins hMSH2 (15) and hMLH1/hPMS2 (16). The functional role of hEXO1 in MMR was addressed in complementation assays (5) as well as in reconstituted systems (17–20). Taken together, the evidence provided by these studies pointed to hEXO1 as the most likely candidate for the excision step during MMR in mammals. In addition to MMR, yeast Exo1 was shown to participate to mitotic (21) and meiotic recombination (2) and to end-resection at telomeres (22). The physical interaction observed in human cells between hEXO1 and the Werner Syndrome helicase WRN (23) and RECQ1 (24) further pointed to a role for hEXO1 in the resolution of DNA intermediates that are formed during recombination (25). In ectopic expression studies, hEXO1 was shown to interact with PCNA via its C-terminal region and the two proteins co-localized at DNA replication foci (26). Proper nuclear localization of hEXO was shown to depend on the sequence $K_{418}RPR_{421}$, which exhibits strong homology to other monopartite nuclear localization sequences (NLS) (27).

The importance of exonuclease 1 is underscored by the phenotype of $Exo1^{-/-}$ mice that displayed reduced survival, sterility and increased susceptibility to the development of lymphomas (28). Analysis of $Exo1^{-/-}$ cells revealed specific defects in MMR leading to elevated microsatellite instability, increased mutation rate at the Hprt locus and abnormal spindle structures in metaphase cells (28). Moreover, Exo1 mutant mice displayed altered somatic hypermutation and reduced class switch recombination (29).

Consistent with its proposed role at sites of DNA replication (30,31), we have previously shown that the hEXO1 protein is selectively destabilized in response to fork arrest. We reported the rapid degradation of hEXO1 to depend on ubiquitin-mediated proteasome pathways and to be facilitated by phosphorylation (32). In the present study, we have examined the pathway transducing the fork-arrest signal to hEXO1 and we have identified ATR as the responsible kinase. Moreover, we have localized the sites of phosphorylation in hEXO1 and assessed their role in the stability of the protein. Finally, we have generated and characterized an antibody to one of the fork arrest-induced sites of phosphorylation in hEXO1 that would represent a useful tool in studies addressing DNA replication fork stalling.

MATERIALS AND METHODS

Antibodies and chemicals

The polyclonal antibody F-15 to the N-terminus of hEXO1 was previously described (32). A monoclonal antibody to full-length EXO1 (Ab-4, clone 266) was purchased from NeoMarkers (Fremont, CA, USA). Antibodies to CHK1-pS_{345}, CHK2-pT_{68} and p53-pS_{15} were from Cell Signaling Technology (Beverly, MA, USA). The antibody to ATM-pS_{1981} was from Rockland (Gilbertsville, PA, USA). Antibodies to ATM and ATR were from Gentex (San Antonio, TX, USA) and Calbiochem (San Diego, CA, USA), respectively. Antibodies to TFIIH (sc-293) and MSH6 (clone 44, G70220) were from Santa Cruz Biotechnology (Santa Cruz, CA, USA) and BD Transduction Laboratories (San Jose, CA, USA), respectively. The Omni-probe antibody (sc-499) used to detect Omni-tagged hEXO1 was from Santa Cruz Biotechnology. HRP-conjugated anti-mouse and anti-rabbit secondary antibodies were obtained from Amersham-Biosciences/GE-Healthcare (Otelfingen, Switzerland), whereas the secondary anti-goat was obtained from Santa Cruz Biotechnology.

The antibody to phosphorylated S_{714} in hEXO1 was raised using the peptide CNIKLLDpSQSDQT, where pS represents phospho-Serine (Eurogentec, Seraing, Belgium). The HPLC purified peptide was coupled to Keyhole Limpet Hemocyanin (KLH) and used to immunize two rabbits. The resulting sera were affinity purified by two consecutive chromatography steps over phosphopeptide and non-phosphopeptide columns. The phospho-specific antibody was eluted with 0.1 M glycine–HCl pH 2.5 and neutralized with 1 M Tris–HCl pH 8.0.

Hydroxyurea (HU) and caffeine were obtained from Sigma (St. Louis, MO, USA) and dissolved in water. KU-55933 was kindly provided by Kudos Pharmaceuticals (Cambridge, UK) and dissolved in DMSO. MG132 was purchased from Calbiochem and dissolved in DMSO.

Expression vectors for wild type (wt) and mutant hEXO1

The protein referred as hEXO1 throughout this study is the isoform b. An expression vector for wt-hEXO1 was created by subcloning full-length hEXO1 in pcDNA3.1-His© (Invitrogen, Carlsbad, CA, USA) 3′ to a His-tag that is specifically recognized by the Omni-probe antibody. Single- and multiple-hEXO1 mutants of the sites of phosphorylation (Ser/Thr > Ala) were generated with the QuikChange site-directed mutagenesis kit (Stratagene, La Jolla, CA, USA) using wt-hEXO1 as template. The overlapping oligonucleotides employed were the following:

S_{454} > A forward: 5′-GCAATAAATCATTGGCCTTTTCTGAAGTG-3′

S_{454} > A reverse: 5′-CACTTCAGAAAAGCCCAATGATTTATTGC-3′

T_{621} > A forward: 5′-GAGATTTTTCAAGAGCGCCGAGCCCCTCTCC-3′

T_{621} > A reverse: 5′-GGAGAGGGGCTCGGCGCTCTTGAAAAATCTC-3′

S_{714} > forward: 5′-GCAATATTAAGTTACTTGACGATCAAAGTGACCAGACC-3′

S_{714} > reverse: 5′-CGTTATAATTCAATGAACTGCTAGTTTCACTGGTCTGG-3′

S_{674} > A forward: 5′-GGCATGTTCTGCACAGTCCCAGGAAAG-3′

S_{674} > A reverse: 5′-CTTTCCTGGGACTGTGCAGAACATGCC-3′

S_{676} > A forward: 5′-GTTCTGCACAGGCCCAGGAAAGTGG-3′

S_{676} > A reverse: 5′-CCACTTTCCTGGGCCTGTGAAGAAC-3′

S_{693} > A forward: 5′-GCATCAAAGCTTGCTCAGTGCTCTAG-3′

S_{693} > A reverse: 5′-CTAGAGCACTGAGCAAGCTTTGATGC-3′

All single and multiple mutations were verified by DNA sequencing.

Cell culture and transfections

HEK-293, HEK-293T, HeLa, U2OS, mouse embryonal fibroblast (MEF) and NIH3T3 cells were maintained in DMEM (OmniLab, Mettmenstetten, Switzerland) supplemented with 10% fetal calf serum (FCS) (Life technologies, Rockville, MD, USA), penicillin (100 U/ml) and streptomycin (100 µg/ml). The ATM-deficient (AT) fibroblasts AT22IJE-T and the matched line complemented with an ATM minigene (AT + ATM) were kindly provided by Y. Shiloh (Tel Aviv University, Israel) and were maintained as described (33). ATR-Seckel cells were kindly provided by M. O'Driscoll and P. Jeggo (University of Sussex, UK) and were maintained in RPMI (OmniLab, Mettmenstetten, Switzerland) supplemented with 15% FCS, penicillin (100 units/ml) and streptomycin (100 µg/ml).

Transient transfections were performed in 6 cm cell culture dishes using 0.5 µg expression vector for wt-EXO1 or Ala-point mutants and the FuGENE-6® transfection reagent (Roche, Basel, Switzerland). Eight hours upon transfection cells were either left untreated or treated with HU for 24 h and harvested 32 h post-transfection.

To create stable cell lines expressing shRNA for ATM or ATR, the constructs described in Ref. (34) were used. HEK-293T cells were transfected either with empty vector (EV) or with shRNA specific to ATM or ATR. Cells underwent selection with 10 µg/ml puromycin for 3 weeks. Downregulation of specific target genes was monitored by western blot analysis.

Irradiation of cell was performed using a Faxitron® Cabinet X-ray system, model 43855D (Faxitron X-ray Corp., Wheeling, IL, USA).

Western blotting and immunoprecipitation

Cellular proteins were extracted using ice-cold lysis buffer (50 mM Tris–HCl pH 7.5, 120 mM NaCl, 20 mM NaF, 1 mM EDTA, 6 mM EGTA, 15 mM Na-pyrophosphate, 0.5 mM Na-orthovanadate, 1 mM benzamidine, 0.1 mM phenylmethylsulfonyl fluoride and 1% nonidet P-40). Protein concentration was determined using the Bio-Rad Protein Assay Reagent (Bio-Rad, Hercules, CA, USA). Detection of proteins by western blot analysis was performed following separation of whole cell extracts (50 µg) on 8% SDS–PAGE. To detect ATM or ATR in whole cell extracts, 6% SDS–PAGE was used. Proteins were transferred to polyvinylidene difluoride (PVDF) (Amersham Biosciences GE-Healthcare, Otelfingen, Switzerland), probed with appropriate antibodies and immune complexes were revealed using the enhanced chemiluminescence system (Amersham Biosciences GE-Healthcare, Otelfingen, Switzerland).

Immunoprecipitation of hEXO1 was carried out with polyclonal antibody F-15, as previously described (32), using HEK-293 (2 mg), HEK-293T (2 mg), HeLa (5 mg), U2OS (7 mg), MEF (6 mg) or NIH3T3 (9 mg) total cell extracts. The immunoprecipitated proteins were revealed by western blot using monoclonal Ab-4 antibody.

Mass spectrometric analysis

HEK-293 cells were transfected with an expression vector for wt-hEXO1 using Metafectene® (Biontex, Planegg, Germany) as transfection reagent. Twenty-four hours upon transfection, cells were either left untreated or treated with HU for 24 h and were harvested 48 h post-transfection. Using the Omni-probe antibody, hEXO1 was immunoprecipitated from 12 mg of cell extracts, for 3 h at 4°C. The antibody was captured on protein G-agarose beads that were subsequently washed twice with TNET buffer (50 mM Tris–HCl pH 7.5, 140 mM NaCl, 5 mM EDTA and 1% Triton X-100) and twice with TNE buffer (50 mM Tris–HCl pH 7.5, 140 mM NaCl and 5 mM EDTA) before boiling in an equal volume of 2× Laemmli-SDS sample buffer. Samples were alkylated with iodoacetamide (55 mM) for 45 min in the dark. Proteins were subjected to electrophoresis on 8% SDS–PAGE and stained with Coomasie Brilliant Blue. Bands corresponding to Omni-hEXO1 were excised and digested with 1 µg trypsin (Promega, Madison, WI, USA) in 50 mM ammonium bicarbonate (pH 8.0) at 37°C for 16 h (35). The resulting peptides were analyzed by capillary liquid chromatography-tandem mass spectrometry (LC–MS/MS) using a Magic C18 100 µm × 10 cm HPLC column (Spectronex, Basel, Switzerland) connected online to an ion-trap Finnigan DecaXP (ThermoFinnigan, San Jose, CA, USA). A linear gradient from 5 to 50% solvent B (0.1% formic acid and 80% (v/v) acetonitrile in water) in solvent A (0.1% formic acid and 2% acetonitrile in water) was delivered in 60 min with a Rheos 2000 HPLC system (Flux, Basel, Switzerland) at 100 µl/min flow rate. A pre-column flow-splitter reduced the flow to ~300 nl/min and the peptides were manually loaded with a 10 µl Hamilton syringe on a peptide cap-trap cartridge (Michrom BioResources, Auburn, CA, USA) mounted in the injection loop of the MS. The eluting peptides were ionized by electrospray ionization, detected and the peptide ions were automatically selected and fragmented by collision-induced dissociation (MS/MS) in the ion trap. Individual MS/MS spectra were compared against the known protein sequence using TurboSequest software (36). Phosphorylated peptides were sequenced more than once.

RESULTS AND DISCUSSION

hEXO1 is phosphorylated in response to fork arrest

Using HEK-293T cells as model system, we have previously shown that the hEXO1 protein is phosphorylated and that inhibitors of DNA replication, but not genotoxic agents, increase the extent of hEXO1 phosphorylation.

This, in turn, results in ubiquitination of hEXO1, which is followed by rapid degradation of the protein in a proteasome-dependent manner (32). To assess whether this is a peculiarity of HEK-293T cells or a common response to agent that stall replication, we analyzed the parental HEK-293 cells along with HeLa, U2OS, MEF and NIH3T3 cells. In all cases, visualization of hEXO1 required immunoprecipitation, as the amount of hEXO1 protein present in total extracts was below the threshold of detection of western blot analysis. This confirmed that hEXO1 is a rare protein in all cell lines examined. Moreover, in all cases treatment with HU led to decrease of hEXO1 protein amount (Figure 1A and Supplementary Figure 1A), as previously reported for HEK-293T cells (32). In order to identify the DNA structure checkpoint pathway that controls phosphorylation of hEXO1, we employed the non-selective PI3K-like kinase inhibitor caffeine as well as the selective ATM inhibitor KU-55933 (37). Addition of caffeine to HEK-293T cells prior to the treatment with HU abolished activation of the ATR-downstream target CHK1 and led to rescue of HU-induced hEXO1 degradation (Figure 1B, compare lane 4 with lane 5). This, however, was not the case when cells were pre-treated with the selective ATM inhibitor KU-55933 (Figure 1B, compare lane 4 with lane 6). In order to assess whether KU-55933 was functional under our assay conditions, we treated HEK-293T cells with the compound prior to administering ionizing radiation (10 Gy) or HU (2 mM). The data showed that whereas KU-55933 was very effective in inhibiting ATM phosphorylation at S_{1981} as well phosphorylation of the downstream effector p53 at S_{15} in response to IR, the inhibitor could not block either of the two events in cells treated with HU (Supplementary Figure 1B). This indicates that the kinase activated in response to HU was ATR. The ATR-dependent phosphorylation of ATM that we observed is in agreement with evidence previously reported in the literature for UV-induced DNA damage (38) and confirms the reported cross-talk between these two PI3K-like kinases (39). To substantiate the finding that ATR controls hEXO1 stability, we examined the effect of down-regulating ATR or ATM by means of RNA interference. The shRNA constructs employed (34) led to a specific, although not compete, reduction of the level of the two PI3K-like kinases (Figure 1C). In this setting, the HU-induced hEXO1 degradation was only rescued upon knocking-down ATR expression. The residual hEXO1 protein upon HU treatment was 35%, 57% or 37% (Figure 1C, lanes 2, 4 and 6, respectively) as compared to the untreated controls. The fact that the rescue of hEXO1 degradation observed in these experiments was partial might depend on the potency of the shRNA to ATR, which appeared to be less effective than the one to ATM (Figure 1C). Quantification of the data indicated that the reduction of protein expression was 75% for ATM and 55% for ATR. In order to get a more definitive answer to the involvement of ATR in the control of hEXO1 stability, we examined the ATR-Seckel cell line. These cells carry a mutated ATR allele that is transcribed in an mRNA undergoing incorrect splicing (40). Nonetheless, ATR-Seckel cells maintain low level of the correctly spliced mRNA for ATR (40) and in the course of culturing, display increasing expression of functional ATR (M. O'Driscoll and P. Jeggo, personal communication). Such model appeared to be ideal to assess the effect of differential level of ATR on hEXO1 stability. In this system, we observed that the expression of hEXO1 was higher in early- than in late-passage cells (Figure 1D, compare lane 1 with lane 3), in a manner that was inversely proportional to the level of expressed ATR. More importantly, treatment of late-passage Seckel cells with HU led to a clear decrease in the amount of hEXO1, an effect that did not occur in early passage cells (Figure 1D, compare lane 4 with lane 2).

To finally confirm the lack of involvement of ATM in signaling to hEXO1, we examined the response of fibroblast derived from an AT-patient (33). Both in ATM-deficient and -proficient fibroblasts, hEXO1 displayed a similar pattern of degradation in response to HU treatment (Figure 1E), thus ruling out a role for ATM in this process. Taken together, these data show that the stalled-fork signal was relayed to hEXO1 through an ATR-dependent pathway.

Identification of the sites of phosphorylation in hEXO1

Having established that hEXO1 was phosphorylated in an ATR-dependent manner in response to stalled forks, we set out to identify the sites of phosphorylation. To this end, we ectopically expressed an Omni-tagged form of hEXO1 in HEK-293 cells. Large-scale immunoprecipitations (Figure 2A) allowed us to obtain sufficient amount of hEXO1 protein to perform LC-MS/MS analysis. In typical experiments, we were able to cover >85% of hEXO1 sequence (Supplementary Figure 2). The results show that hEXO1 was phosphorylated at nine residues (8 Ser, 1 Thr) under basal conditions and at three additional sites (2 Ser, 1 Thr) upon HU treatment (Table 1, Figure 2B and Supplementary Figure 2). The three HU-induced sites of phosphorylation (S_{454}, T_{621} and S_{714}) conformed to the requirement for recognition by CHK1/CHK2, MAPK/SAPK and ATM/ATR, respectively. These findings point to the involvement of classic DNA damage signaling pathways as well as stress-activated kinase cascades in hEXO1 phosphorylation in response to HU. Among the nine basal sites of phosphorylation, residues S_{376}, S_{598}, S_{623} and S_{639} conformed to the recognition by proline-directed kinases (S/T-P), whereas residues T_{581} and S_{660} resembled typical CK2 targets (S/T-X_{1-2}-D/E). The sites S_{422} and S_{746} fulfilled the requirement for phosphorylation by CHK1/CHK2 (Φ-X-K/R-X_2-S/T, where Φ is any hydrophobic amino acid), or, as second choice, for CK2. Among the basal sites of phosphorylation that we identified is S_{598}, a site that was previously described in a large-scale study on HeLa cell nuclear phosphoproteome (41). A representative MS-chromatogram for the identification of phosphorylation at the HU-induced S_{714} site is shown in Supplementary Figure 3.

Characterization of pS_{714} antibody

In order to monitor hEXO1 phosphorylation in response to inhibition of DNA synthesis, we raised a rabbit polyclonal antibody to pS_{714}. This site is particularly

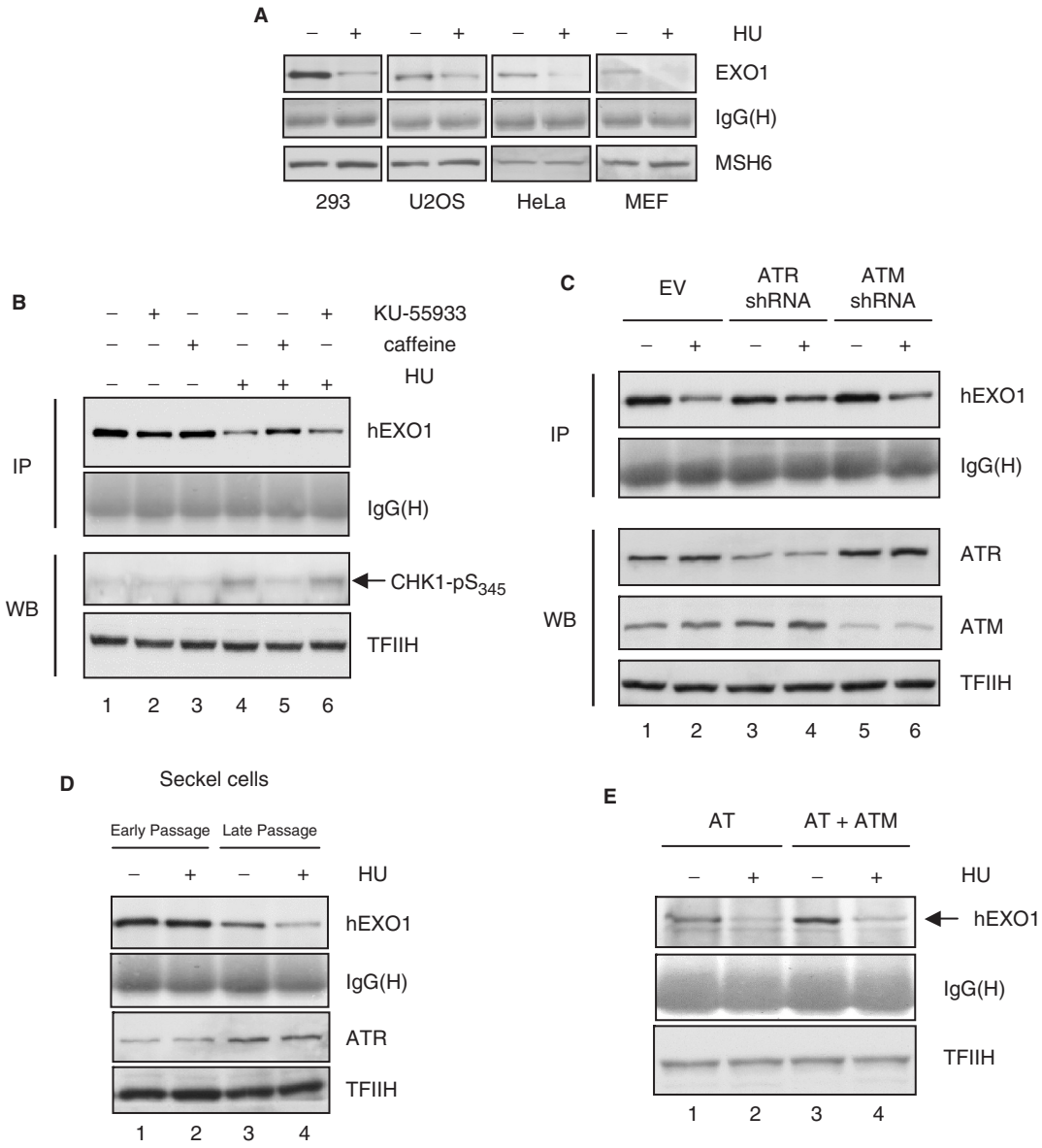

Figure 1. ATR-dependent control of hEXO1 stability in response to stalled replication. (**A**) HEK-293, U2OS, HeLa and MEF cells were grown in the presence or the absence of 2 mM HU for 24 h. Whole cell extracts were immunoprecipitated with the rabbit polyclonal antibody F-15 and resolved on a 8% SDS–PAGE. Human and mouse EXO1 were visualized with the monoclonal antibody Ab-4. MSH6 and IgG(H) were used as controls for the input and the quality of the immunoprecipitation, respectively. (**B**) Upper panels: immunoprecipitation of hEXO1 from HEK-293T cells left untreated (lane 1) or treated for 8 h with either 10 μM KU-55933 (lane 2), 4 mM caffeine (lane 3), 2 mM HU (lane 4), 4 mM caffeine followed by 2 mM HU (lane 5) or 10 μM KU-55933 followed by 2 mM HU (lane 6). hEXO1 was detected as described above. The signal given by IgG(H) was used as control for the quality of the immunoprecipitation. Lower panels: western blot analysis of phosphorylated CHK1 in whole cell extracts was used as read-out for the cellular response to HU. TFIIH was used as loading control. (**C**) HEK-293T cells were stably transfected with EV, ATR or ATM shRNA constructs. hEXO1 was immunoprecipitated from cells left untreated or treated with HU for 16 h. The signal given by IgG(H) was used as control for the quality of the immunoprecipitation. ATR and ATM expression was monitored to assess the extent of downregulation by shRNA. TFIIH served as loading control. The data shown represent one of three independent experiments. (**D**) ATR-Seckel cells at early or late passages were either left untreated or treated with HU for 16 h. hEXO1 was immunoprecipitated as described above. TFIIH and IgG(H) were used as controls for the input and the quality of the immunoprecipitation, respectively. The expression of ATR was examined by western blot analysis. (**E**) AT or AT + ATM fibroblasts were treated in the presence or the absence of HU and the expression of hEXO1 was assessed following immunoprecipitation as described above. TFIIH and IgG(H) were used as controls for input and quality of the immunoprecipitation, respectively.

interesting because it fulfills the requirements for recognition and phosphorylation by ATM/ATR protein kinases and because its phosphorylation has been independently confirmed by large-scale mass spectrometry studies (42) in the course of our work. To assess its specificity, the antibody was tested on total cell extracts derived from HeLa cells that ectopically expressed hEXO1 and were either left untreated or treated with HU. The data indicate that the pS_{714} antibody selectively detected phosphorylated hEXO1 from extracts of HU-treated cells

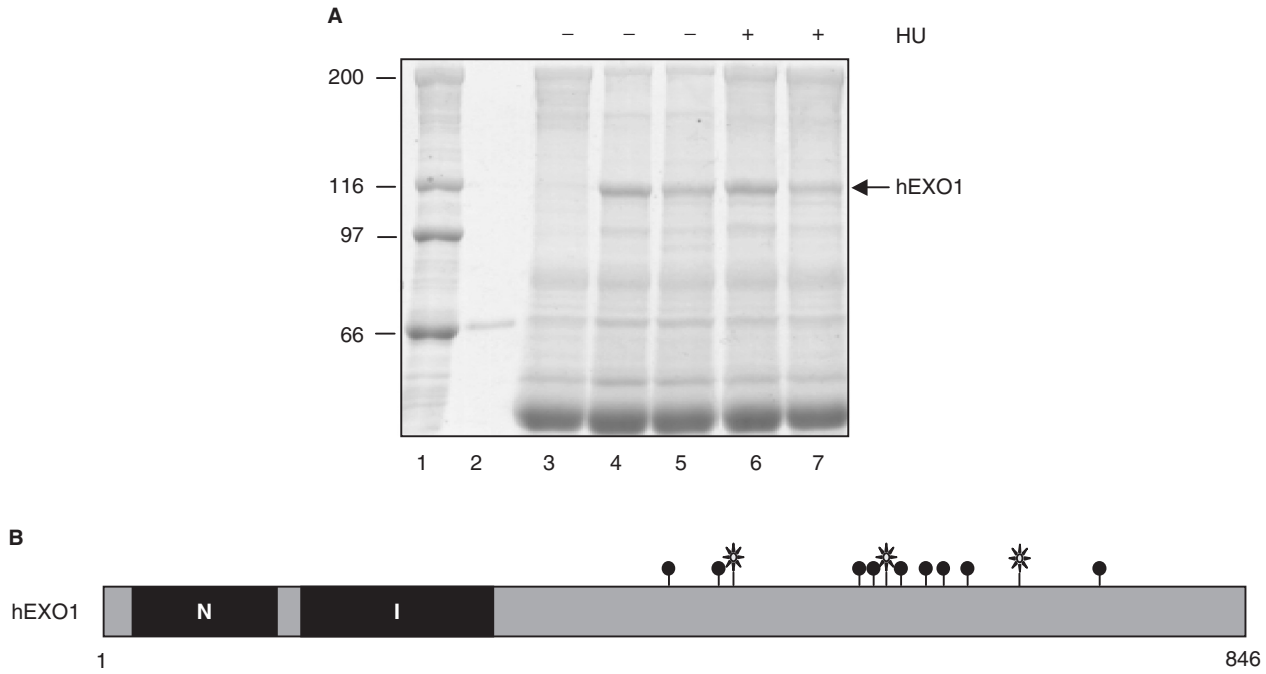

Figure 2. Identification of the sites of phosphorylation in hEXO1. (**A**) HEK-293 cells were transfected with EV (lane 3) or an expression vector encoding Omni-hEXO1 (lanes 4–7). Cells were left untreated (lanes 4 and 5) or treated with 2 mM HU for 24 h (lanes 6 and 7). hEXO1 was immmunoprecipitated with the Omni-probe antibody. Samples were subjected to 8% SDS–PAGE electrophoresis and the gel was stained with Coomassie Brilliant Blue. Molecular weight protein markers (lane 1) and 500 ng BSA (lane 2) were loaded to estimate the amount of immunoprecipitated hEXO1. The protein bands corresponding to hEXO1 were excised from the gel and underwent LC-MS/MS analysis. (**B**) Schematic representation of hEXO1 and localization of the sites of phosphorylation identified by LC-MS/MS. N-terminal (N) and internal (I) catalytic domains are indicated. Dots, basal sites; stars, HU-induced sites.

Table 1. Sites of phosphorylation that were identified in hEXO1 phosphopeptides present among the peptides detected in LC–MS/MS analysis

Phosphopeptide	Phospho-site	Treatment
HRNY**pS**PRPE	Ser_{376}	None
KRPR**pS**AELS	Ser_{422}	None
ATVF**pT**DEES	Thr_{581}	None
TRTI**pS**PPTL	Ser_{598}	None
SRTP**pS**PSPS	Ser_{623}	None
RKSD**pS**PTSL	Ser_{639}	None
SEES**pS**DDES	Ser_{660}	None
GACS**pS**QSQE	Ser_{674}	None
YKSS**pS**ADSL	Ser_{746}	None
NKSL**pS**FSEV	Ser_{454}	HU
DSFR**pT**PSPS	Thr_{621}	HU
KLLD**pS**QSDQ	Ser_{714}	HU

(Figure 3A, upper panel, lane 3), despite the reduction of total hEXO1 amount induced by HU (Figure 3A, middle panel, lane 3 versus lane 2).

To definitely assess whether the epitope recognized by the antibody was phospho-S_{714}, we ectopically expressed wt-hEXO1 or the point mutant A_{714}-hEXO1 in HEK293 cells that were either left untreated or treated with HU. The results obtained show that the pS_{714} antibody could detect the HU-induced increase in hEXO1 phosphorylation only in the case of wt-hEXO1 (Figure 3B, lane 3) but not in the A_{714} point mutant (Figure 3B, lane 4). This allowed us concluding that the pS_{714} antibody specifically reacted with hEXO1 phosphorylated at S_{714}.

Next, we examined the ability of the pS_{714} antibody to detect endogenous hEXO1. To this end, immunoprecipitation experiments were performed on total extracts of HEK-293T cells using either the pS_{714} antibody (Figure 3C, upper panel) or antibody F15 (Figure 3C, lower panel). The data show that antibody pS_{714} was able to precipitate the phosphorylated form of the endogenous hEXO1 protein and this occurred only in the case of HU-treated cells (Figure 3C, lanes 2 and 3). The fact that a higher amount of phosphorylated hEXO1 was precipitated from MG-132 treated cells in comparison to untreated cells (Figure 3C, upper panel, lane 3 versus lane 2), confirmed our early finding that hEXO1 degradation is phosphorylation-dependent (32). Antibody pS_{714} was also suitable for the detection of phosphorylated hEXO1 by western blot analysis upon immunoprecipitation of the endogenous protein. A weak but clear signal was observed upon treatment with HU and the proteasome inhibitor MG-132 to prevent hEXO1 degradation (Supplementary Figure 4).

Finally, considering that S_{714} belongs to the S/T-Q type of DNA damage sites, we asked whether S_{714} is specifically phosphorylated upon replication fork stalling or if it is also targeted in response to other types of DNA damage. To this end, we treated HEK-293T cells ectopically expressing Omni-tagged hEXO1 with either IR or HU. Detection of hEXO1 with the pS_{714} antibody indicated that HU potently induced phosphorylation at this site (Figure 3D,

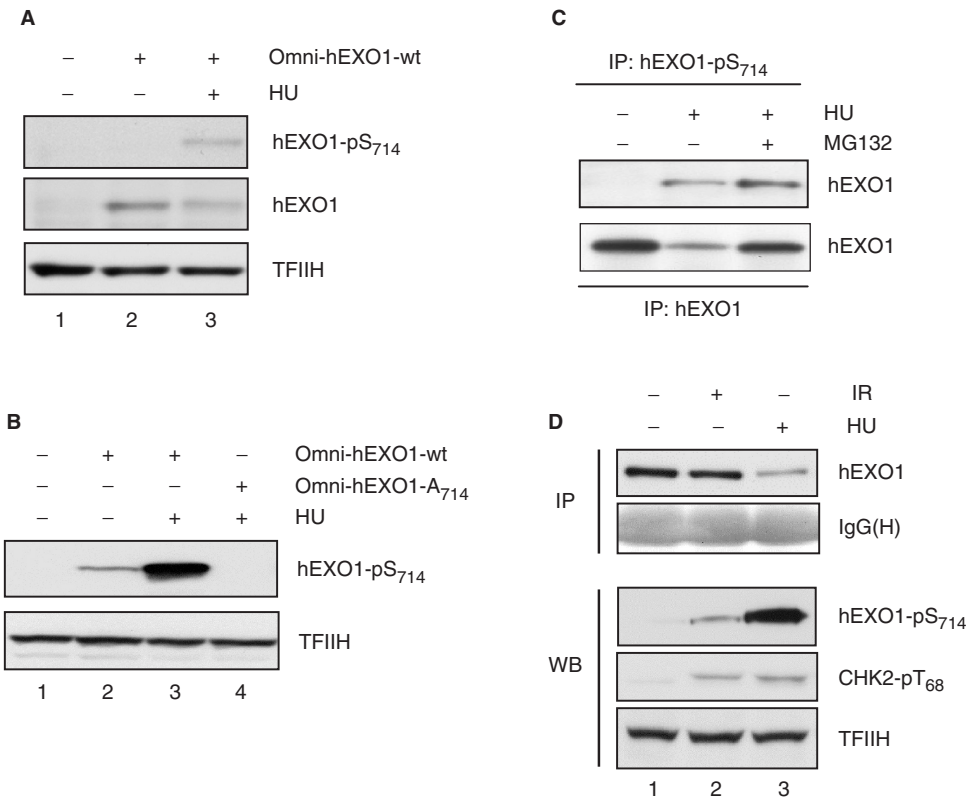

Figure 3. Characterization of the hEXO1-pS$_{714}$ antibody. (**A**) HeLa cells were transfected with EV (lane 1) or Omni-hEXO1 expression vector (lanes 2 and 3). Cells were left untreated or treated with HU for 24 h. Whole cell extracts were subjected to 8% SDS–PAGE electrophoresis, followed by western blot analysis using antibody pS$_{714}$ to detect phosphorylated hEXO1 (upper panel) or mouse monoclonal antibody Ab-4 to visualize the entire pool of hEXO1 (middle panel). TFIIH served as control for equal loading. (**B**) HEK-293T cells were transfected with EV (lane 1), expression vector for wild-type Omni-hEXO1 (lanes 2 and 3) or for the non-phosphorylatable mutant Omni-hEXO1-A$_{714}$ (lane 4). Cells were treated with HU as indicated. Western blot analysis of total cell extracts was performed using antibody pS$_{714}$. (**C**) Immunoprecipitation of endogenous hEXO1 from HEK-293T cells using either pS$_{714}$ antibody (upper panel) or rabbit polyclonal antibody F-15 (lower panel) followed by western blot analysis with mouse monoclonal antibody Ab-4. (**D**) HEK-293T cells were transfected with an expression vector for wild-type Omni-hEXO1 (lanes 1–3). Cells were left untreated or treated with IR (10 Gy) or HU (2 mM), as indicated, and hEXO1 was immunoprecipitated using rabbit polyclonal antibody F-15 (upper panels). The signal given by IgG(H) was used as control for the quality of the immunoprecipitation. The phosphorylation status of hEXO1 and CHK2 was monitored by western blot analysis using phospho-specific antibodies (lower panels). TFIIH was used as loading control.

lane 3), whereas the IR treatment was only minimally affecting phosphorylation at S$_{714}$ (Figure 3D, lane 2).

Taken together, these results show that the pS$_{714}$ antibody is able to specifically recognize the phosphorylated S$_{714}$ epitope in hEXO1 and that S$_{714}$ is a site selectively targeted in response to stalled replication. The pS$_{714}$ antibody may be potentially employed to monitor the flow of signal transduction events in studies on stalled DNA replication. A second foreseeable application for this tool is the identification of hEXO1 interacting proteins by means of combined immunoprecipitation/mass spectrometry under conditions of stalled DNA replication, when hEXO1 is phosphorylated at S$_{714}$.

Mutation of the sites of phosphorylation and effect on hEXO1 protein stability

In order to assess the impact of phosphorylation on hEXO1 protein stability, we generated single and multiple Alanine point mutants of the sites of phosphorylation and expressed them in HeLa cells. The data showed that single mutation of the three HU-induced sites (A$_{454}$, A$_{621}$ and A$_{714}$) did not rescue hEXO1 degradation in response to HU (Figure 4A). Likewise, the double point mutants A$_{621,714}$ and A$_{454,714}$ were as sensitive as wild-type hEXO1 to the effect of HU (Figure 4B). On the contrary, the triple mutant A$_{454,621,714}$ was expressed to an apparently higher level than wild-type hEXO1 and resulted to be less sensitive to HU (Figure 4B). The higher basal stability of the A$_{454,621,714}$ mutant is unlikely to result from constitutively increased expression (i.e. transcription and translation) of this specific isoform as compared to other point mutants. Such increased stability rather reflects the fact that, although phosphorylation at the three HU-induced sites might be substoichiometric under basal conditions of cell growth, it is sufficient to trigger continuous degradation of hEXO1. Support to this view comes from the evidence that low level of phosphorylation at S$_{714}$ was detected with the pS$_{714}$ antibody in exponentially growing HEK-293T cells that were ectopically expressing hEXO1 but were not treated with HU (Figure 3B, upper panel, lane 2). As mentioned above, we observed that the triple mutant A$_{454,621,714}$ displayed

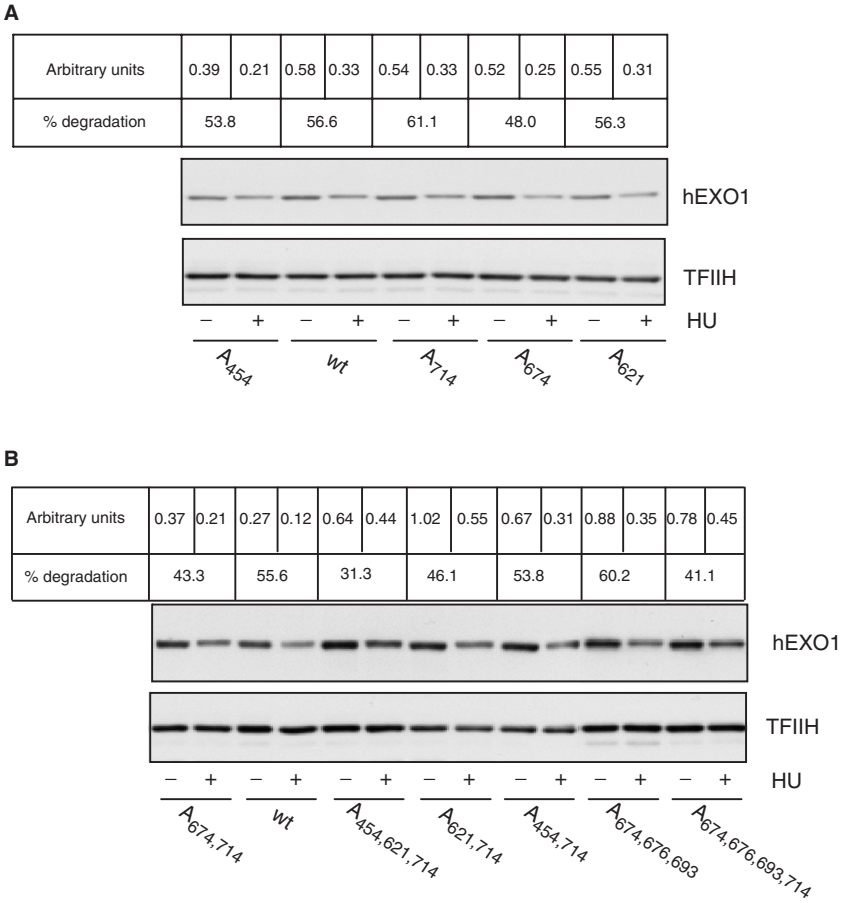

Figure 4. Effect of HU on non-phosphorylatable hEXO1 mutants. (**A**) HeLa cells were transfected with an expression vector for wild-type Omni-hEXO1 or the single Ala point mutants indicated in the panel. Cells were left untreated or treated with HU for 24 h. Total cell extracts were analyzed by western blot using the Omni-probe antibody to detect the tagged hEXO1 protein. Data were quantified using ImageQuant 5.2 software (Amersham-Biosciences/GE-Healthcare). Percent degradation was calculated as the ratio between the amount of protein present in HU treated over untreated lanes. TFIIH was used for normalization. (**B**) Analysis of multiple hEXO1-Ala point mutants was performed as indicated above. The data shown in panels A and B represent one of three independent experiments.

increased resistance to HU-induced degradation as compared to wt-hEXO1 ($29.3 \pm 6.35\%$ degradation for the triple mutant versus $53.7 \pm 10.69\%$ for the wild type, Supplementary Figure 5). On the other hand, mutation of all sites in a S/T-Q cluster (Supplementary Figure 2), did not result in any significant rescue of hEXO1 degradation (Figure 4B). Taken together, these data indicate that the HU-induced phosphorylation of hEXO1 at the three residues described in this study facilitated the destabilization of the protein, though additional events may contribute to hEXO1 degradation in response to fork arrest. With regard to this point, it is worth considering the possibility that ATR-dependent phosphorylation of hEXO1 interacting partners, among which might be a specific E3-ligase for hEXO1, could be of key importance in the overall control of hEXO1 degradation in response to stalled replication. Future experiments will aim at clarifying this issue.

SUPPLEMENTARY DATA

Supplementary Data are available at NAR Online.

ACKNOWLEDGEMENTS

We are indebted to C.M. Azzalin and J. Lengner (ISREC, Lausanne, Switzerland) for providing shRNA constructs, KUDOS Pharmaceuticals (Cambridge, UK) for supplying the ATM inhibitor KU-55933 and M. O'Driscoll and P. Jeggo, University of Sussex, UK for providing Seckel cells. We would like to thank members of S.F. laboratory for helpful suggestions. M.E.-S. was supported by a Swiss National Science Foundation grant (31-100090/1) and by a grant from the Sassella-Foundation, Zurich, Switzerland to S.F. We are also indebted to the Désirée and Niels Yde Foundation and the Ida De Pottère-Leupold-Fonds for generous financial support. Funding to pay the Open Access publication charges for this article was provided by Swiss National Science Foundation.

Conflict of interest statement. None declared.

REFERENCES

1. Szankasi,P. and Smith,G.R. (1992) A DNA exonuclease induced during meiosis of Schizosaccharomyces pombe. *J. Biol. Chem.*, **267**, 3014–3023.

2. Tsubouchi,H. and Ogawa,H. (2000) Exo1 roles for repair of DNA double-strand breaks and meiotic crossing over in Saccharomyces cerevisiae. *Mol. Biol. Cell*, **11**, 2221–2233.
3. Digilio,F.A., Pannuti,A., Lucchesi,J.C., Furia,M. and Polito,L.C. (1996) Tosca: a Drosophila gene encoding a nuclease specifically expressed in the female germline. *Dev. Biol.*, **178**, 90–100.
4. Lee,B.I., Shannon,M., Stubbs,L. and Wilson,D.M.III (1999) Expression specificity of the mouse exonuclease 1 (mExo1) gene. *Nucleic Acids Res.*, **27**, 4114–4120.
5. Tishkoff,D.X., Amin,N.S., Viars,C.S., Arden,K.C. and Kolodner,R.D. (1998) Identification of a human gene encoding a homologue of Saccharomyces cerevisiae EXO1, an exonuclease implicated in mismatch repair and recombination. *Cancer Res.*, **58**, 5027–5031.
6. Tishkoff,D.X., Boerger,A.L., Bertrand,P., Filosi,N., Gaida,G.M., Kane,M.F. and Kolodner,R.D. (1997) Identification and characterization of Saccharomyces cerevisiae EXO1, a gene encoding an exonuclease that interacts with MSH2. *Proc. Natl Acad. Sci. USA*, **94**, 7487–7492.
7. Qiu,J., Qian,Y., Chen,V., Guan,M.X. and Shen,B. (1999) Human exonuclease 1 functionally complements its yeast homologues in DNA recombination, RNA primer removal, and mutation avoidance. *J. Biol. Chem.*, **274**, 17893–17900.
8. Rasmussen,L.J., Rasmussen,M., Lee,B., Rasmussen,A.K., Wilson,D.M.III, Nielsen,F.C. and Bisgaard,H.C. (2000) Identification of factors interacting with hMSH2 in the fetal liver utilizing the yeast two-hybrid system. In vivo interaction through the C-terminal domains of hEXO1 and hMSH2 and comparative expression analysis. *Mutat. Res.*, **460**, 41–52.
9. Wilson,D.M.III, Carney,J.P., Coleman,M.A., Adamson,A.W., Christensen,M. and Lamerdin,J.E. (1998) Hex1: a new human Rad2 nuclease family member with homology to yeast exonuclease 1. *Nucleic Acids Res.*, **26**, 3762–3768.
10. Lee,B.I. and Wilson,D.M.III (1999) The RAD2 domain of human exonuclease 1 exhibits 5′ to 3′ exonuclease and flap structure-specific endonuclease activities. *J. Biol. Chem.*, **274**, 37763–37769.
11. Szankasi,P. and Smith,G.R. (1995) A role for exonuclease I from S. pombe in mutation avoidance and mismatch correction. *Science*, **267**, 1166–1169.
12. Lynch,H.T. and de la Chapelle,A. (2003) Hereditary colorectal cancer. *N. Engl. J. Med.*, **348**, 919–932.
13. Tran,P.T., Simon,J.A. and Liskay,R.M. (2001) Interactions of Exo1p with components of MutLalpha in Saccharomyces cerevisiae. *Proc. Natl Acad. Sci. USA*, **98**, 9760–9765.
14. Amin,N.S., Nguyen,M.N., Oh,S. and Kolodner,R.D. (2001) exo1-Dependent mutator mutations: model system for studying functional interactions in mismatch repair. *Mol. Cell. Biol.*, **21**, 5142–5155.
15. Schmutte,C., Marinescu,R.C., Sadoff,M.M., Guerrette,S., Overhauser,J. and Fishel,R. (1998) Human exonuclease I interacts with the mismatch repair protein hMSH2. *Cancer Res.*, **58**, 4537–4542.
16. Schmutte,C., Sadoff,M.M., Shim,K.S., Acharya,S. and Fishel,R. (2001) The interaction of DNA mismatch repair proteins with human exonuclease I. *J. Biol. Chem.*, **276**, 33011–33018.
17. Genschel,J., Bazemore,L.R. and Modrich,P. (2002) Human exonuclease I is required for 5′ and 3′ mismatch repair. *J. Biol. Chem.*, **277**, 13302–13311.
18. Genschel,J. and Modrich,P. (2003) Mechanism of 5′-directed excision in human mismatch repair. *Mol. Cell*, **12**, 1077–1086.
19. Dzantiev,L., Constantin,N., Genschel,J., Iyer,R.R., Burgers,P.M. and Modrich,P. (2004) A defined human system that supports bidirectional mismatch-provoked excision. *Mol. Cell*, **15**, 31–41.
20. Kadyrov,F.A., Dzantiev,L., Constantin,N. and Modrich,P. (2006) Endonucleolytic function of MutLalpha in human mismatch repair. *Cell*, **126**, 297–308.
21. Fiorentini,P., Huang,K.N., Tishkoff,D.X., Kolodner,R.D. and Symington,L.S. (1997) Exonuclease I of Saccharomyces cerevisiae functions in mitotic recombination in vivo and in vitro. *Mol. Cell. Biol.*, **17**, 2764–2773.
22. Maringele,L. and Lydall,D. (2002) EXO1-dependent single-stranded DNA at telomeres activates subsets of DNA damage and spindle checkpoint pathways in budding yeast yku70Delta mutants. *Genes Dev.*, **16**, 1919–1933.
23. Sharma,S., Sommers,J.A., Driscoll,H.C., Uzdilla,L., Wilson,T.M. and Brosh,R.M.Jr (2003) The exonucleolytic and endonucleolytic cleavage activities of human exonuclease 1 are stimulated by an interaction with the carboxyl-terminal region of the Werner syndrome protein. *J. Biol. Chem.*, **278**, 23487–23496.
24. Doherty,K.M., Sharma,S., Uzdilla,L.A., Wilson,T.M., Cui,S., Vindigni,A. and Brosh,R.M.Jr (2005) RECQ1 helicase interacts with human mismatch repair factors that regulate genetic recombination. *J. Biol. Chem.*, **280**, 28085–28094.
25. Tran,P.T., Erdeniz,N., Symington,L.S. and Liskay,R.M. (2004) EXO1-A multi-tasking eukaryotic nuclease. *DNA Repair*, **3**, 1549–1559.
26. Nielsen,F.C., Jager,A.C., Lutzen,A., Bundgaard,J.R. and Rasmussen,L.J. (2004) Characterization of human exonuclease 1 in complex with mismatch repair proteins, subcellular localization and association with PCNA. *Oncogene*, **23**, 1457–1468.
27. Knudsen,N.O., Nielsen,F.C., Vinther,L., Bertelsen,R., Holten-Andersen,S., Liberti,S.E., Hofstra,R., Kooi,K. and Rasmussen,L.J. (2007) Nuclear localization of human DNA mismatch repair protein exonuclease 1 (hEXO1). *Nucleic Acids Res.*, **35**, 2609–2619.
28. Wei,K., Clark,A.B., Wong,E., Kane,M.F., Mazur,D.J., Parris,T., Kolas,N.K., Russell,R., Hou,H.Jr *et al.* (2003) Inactivation of Exonuclease 1 in mice results in DNA mismatch repair defects, increased cancer susceptibility, and male and female sterility. *Genes Dev.*, **17**, 603–614.
29. Bardwell,P.D., Woo,C.J., Wei,K., Li,Z., Martin,A., Sack,S.Z., Parris,T., Edelmann,W. and Scharff,M.D. (2004) Altered somatic hypermutation and reduced class-switch recombination in exonuclease 1-mutant mice. *Nat. Immunol.*, **5**, 224–229.
30. Sogo,J.M., Lopes,M. and Foiani,M. (2002) Fork reversal and ssDNA accumulation at stalled replication forks owing to checkpoint defects. *Science*, **297**, 599–602.
31. Cotta-Ramusino,C., Fachinetti,D., Lucca,C., Doksani,Y., Lopes,M., Sogo,J. and Foiani,M. (2005) Exo1 processes stalled replication forks and counteracts fork reversal in checkpoint-defective cells. *Mol. Cell*, **17**, 153–159.
32. El-Shemerly,M., Janscak,P., Hess,D., Jiricny,J. and Ferrari,S. (2005) Degradation of human exonuclease 1b upon DNA synthesis inhibition. *Cancer Res.*, **65**, 3604–3609.
33. Ziv,Y., Bar-Shira,A., Pecker,I., Russell,P., Jorgensen,T.J., Tsarfati,I. and Shiloh,Y. (1997) Recombinant ATM protein complements the cellular A-T phenotype. *Oncogene*, **15**, 159–167.
34. Azzalin,C.M. and Lingner,J. (2006) The human RNA surveillance factor UPF1 is required for S phase progression and genome stability. *Curr. Biol.*, **16**, 433–439.
35. Shevchenko,A., Wilm,M., Vorm,O. and Mann,M. (1996) Mass spectrometric sequencing of proteins silver-stained polyacrylamide gels. *Anal. Chem.*, **68**, 850–858.
36. Gatlin,C.L., Eng,J.K., Cross,S.T., Detter,J.C. and Yates,J.R.III (2000) Automated identification of amino acid sequence variations in proteins by HPLC/microspray tandem mass spectrometry. *Anal. Chem.*, **72**, 757–763.
37. Hickson,I., Zhao,Y., Richardson,C.J., Green,S.J., Martin,N.M., Orr,A.I., Reaper,P.M., Jackson,S.P., Curtin,N.J. *et al.* (2004) Identification and characterization of a novel and specific inhibitor of the ataxia-telangiectasia mutated kinase ATM. *Cancer Res.*, **64**, 9152–9159.
38. Stiff,T., Walker,S.A., Cerosaletti,K., Goodarzi,A.A., Petermann,E., Concannon,P., O'Driscoll,M. and Jeggo,P.A. (2006) ATR-dependent phosphorylation and activation of ATM in response to UV treatment or replication fork stalling. *EMBO J.*, **25**, 5775–5782.
39. Myers,J.S. and Cortez,D. (2006) Rapid activation of ATR by ionizing radiation requires ATM and Mre11. *J. Biol. Chem.*, **281**, 9346–9350.
40. O'Driscoll,M., Ruiz-Perez,V.L., Woods,C.G., Jeggo,P.A. and Goodship,J.A. (2003) A splicing mutation affecting expression of ataxia-telangiectasia and Rad3-related protein (ATR) results in Seckel syndrome. *Nat. Genet.*, **33**, 497–501.
41. Beausoleil,S.A., Jedrychowski,M., Schwartz,D., Elias,J.E., Villen,J., Li,J., Cohn,M.A., Cantley,L.C. and Gygi,S.P. (2004) Large-scale characterization of HeLa cell nuclear phosphoproteins. *Proc. Natl Acad. Sci. USA*, **101**, 12130–12135.
42. Matsuoka,S., Ballif,B.A., Smogorzewska,A., McDonald,E.R.III, Hurov,K.E., Luo,J., Bakalarski,C.E., Zhao,Z., Solimini,N. *et al.* (2007) ATM and ATR substrate analysis reveals extensive protein networks responsive to DNA damage. *Science*, **316**, 1160–1166.